Propagation inhibition and localization of electromagnetic waves in two-dimensional random dielectric systems

Bikash C. Gupta,* Chao-Hsien Kuo, and Zhen Ye†
Wave Phenomena Laboratory, Department of Physics, National Central University, Chungli, Taiwan 32054, Republic of China
(Received 16 January 2004; revised manuscript received 8 April 2004; published 17 June 2004)

We rigorously calculate the propagation and scattering of electromagnetic waves by rectangular and random arrays of dielectric cylinders in a uniform medium. For regular arrays, the band structures are computed and complete bandgaps are discovered. For random arrays, the phenomenon of wave transmission and scattering is investigated and compared in two scenarios: (1) Wave propagating through the array of cylinders; this is the scenario which has been commonly considered in the literature, and (2) wave transmitted from a source located inside the ensemble. We show that within complete band gaps, results from the two scenarios are similar. Outside the gaps, however, there could be a distinct difference, that is, wave transmission can be inhibited by disorders in the first scenario, but such an inhibition may not prevail in the second scenario.

DOI: 10.1103/PhysRevE.69.066615 PACS number(s): 42.25.Hz, 71.55.Jv

I. INTRODUCTION

More than two decades have passed since the phenomenon of wave localization was explored for propagation of electromagnetic (EM) waves in random media. During this period, a great body of literature has been generated [1]. And the interest in the subject continues to grow even further in recent years [2–10].

With this paper, we present a rigorous study of EM wave scattering and propagation in media containing many dielectric cylinders. The approach is based upon the self-consistent theory of multiple scattering [11] and has been used previously to study acoustic localization in liquid media [9,10] and acoustic attenuation by rigid cylinders in air. [12] In this approach, wave propagation is expressed by a set of coupled exact equations and is solved rigorously. We show that wave localization can be achieved in ranges of frequencies, coincident with yet wider than the complete bandgap. In particular, we compare two scenarios: (1) Wave propagating through arrays array of cylinders, and (2) wave transmitted from a source located inside the ensemble. We show that within complete band gaps, results from the two scenarios are similar, whereas there is a fundamental difference between the two situations when the frequency is outside the gap. Moreover, when localized, not only are waves confined near the transmitting source but a unique collective phenomenon emerges, illustrated by a phase diagram in analogy to the acoustic system [9,10].

II. THE FORMULATION AND SYSTEM

The system considered here is similar to what has been presented in Ref. [4]. Assume that N uniform dielectric cylinders of radius a are placed in parallel in a uniform medium, perpendicular to the x-y plane. The arrangement can be either random or regular. For brevity, we only consider the case of the E-polarization, i.e., the E-field parallel to the z-direction. The qualitative features for both E- and H-polarizations are similar. The scattering and propagation of EM waves can be solved by using the standard multiple scattering theory [11]. When the cylinders are arranged in a regular lattice, the band structure can be computed by the standard plane wave expansion method.

A unit pulsating line source transmitting monochromatic waves is placed at a certain position. The scattered wave from each cylinder is a response to the total incident wave, which is composed of the direct contribution from the source and the multiply scattered waves from each of the other cylinders. The response function of a single cylinder is readily obtained in the form of the partial waves by invoking the usual boundary conditions across the cylinder surface. The total wave (E) at any space point is the sum of the direct wave (E_0) from the transmitting source and the scattered wave from all the cylinders. The normalized field is defined as $T \equiv E/E_0$; thus the trivial geometrical spreading effect is eliminated. The normalized intensity of the wave is represented by the square of the wave field $|T|^2$.

For the reader's convenience, we present briefly the general multiple scattering theory. Consider that N straight cylinders of radius a^i located at $\vec{r}_i$ with $i=1,2,\ldots,N$ to form an array. A line source transmitting monochromatic waves is placed at $\vec{r}_s$. Here we take the standard approach with regard to the source. That is, the transmission from the source is calculated from the multiple scattering theory, and assume that the source is not affected by the surroundings. If some other sources such as a line of atoms are used, the reaction between the source and the backscattered waves should be taken into account.

The scattered wave from the jth cylinder can be written as

$$p_s(\vec{r},\vec{r}_j) = \sum_{n=-\infty}^{\infty} i\pi A_n^j H_n^{(1)}(k|\vec{r}-\vec{r}_j|)e^{in\phi_{\vec{r}-\vec{r}_j}}, \qquad (1)$$

where k is the wavenumber in the medium, $H_n^{(1)}$ is the nth order Hankel function of first kind, and $\phi_{\vec{r}-\vec{r}_j}$ is the azimuthal

*Current address: Department of Physics, University of Illinois, Chicago, IL 60607.
†Request for additional materials could be addressed to the corresponding author Z. Ye at zhen@phy.ncu.edu.tw

angle of the vector $\vec{r}-\vec{r}_j$ relative to the positive x axis. The total incident wave around the ith cylinder ($i=1,2,\ldots,N; i \neq j$) is the summation of the direct incident wave from the source and the scattered waves from all other scatterers, can be expressed as

$$p_{in}^i(\vec{r}) = \sum_{n=-\infty}^{\infty} B_n^i J_n(k|\vec{r}-\vec{r}_i|)e^{in\phi_{\vec{r}-\vec{r}_i}}. \quad (2)$$

In this paper, p stands for the electrical field in the TM mode and the magnetic field in the TE mode.

The coefficients A_n^i and B_n^i can be solved by expressing the scattered wave $p_s(\vec{r},\vec{r}_j)$, for each $j \neq i$, in terms of the modes with respect to the ith scatterer by the addition theorem for Bessel function. Then the usual boundary conditions are matched at the surface of each scattering cylinder. This leads to

$$B_n^i = S_n^i + \sum_{j=1, j\neq i}^{N} C_n^{j,i}, \quad (3)$$

with

$$S_n^i = i\pi H_{-n}^{(1)}(k|\vec{r}_i|)e^{-in\phi_{\vec{r}_i}}, \quad (4)$$

$$C_n^{j,i} = \sum_{l=-\infty}^{\infty} i\pi A_l^j H_{l-n}^{(1)}(k|\vec{r}_i-\vec{r}_j|)e^{i(l-n)\phi_{\vec{r}_i-\vec{r}_j}}, \quad (5)$$

and

$$B_n^i = i\pi\tau_n^j A_n^i, \quad (6)$$

where τ_n^j are the transfer matrices relating the properties of the scatterers and the surrounding medium and are given as

$$\tau_n^j = \frac{H_n^{(1)}(ka^i)J_n'(ka^i/h^i) - g^i h^i H_n^{(1)'}(ka^i)J_n(ka^i/h^i)}{g^i h^i J_n'(ka^i)J_n(ka^i/h^i) - J_n(ka^i)J_n'(ka^i/h^i)}, \quad (7)$$

where

$$h^i = \frac{1}{\sqrt{\epsilon^i}}, \quad \text{and } g^i = \begin{cases} \epsilon^i & \text{for TE waves} \\ 1 & \text{for TM waves} \end{cases},$$

in which ϵ^i is the dielectric constant ratio between the ith scatterer and the surrounding medium.

The coefficients A_n^i and B_n^j can then be inverted from Eq. (3). Once the coefficients A_n^i are determined, the transmitted wave at any spatial point is given by

$$p(\vec{r}) = p_0(\vec{r}) + p_s(\vec{r}) \equiv p_0(\vec{r}) + \sum_{i=1}^{N}\sum_{n=-\infty}^{\infty} i\pi A_n^i H_n^{(1)}(k|\vec{r}-\vec{r}_i|)e^{in\phi_{\vec{r}-\vec{r}_i}}, \quad (8)$$

where p_0 is the field when no scatterers are present, the second term p_s represents the scattered waves. The transmitted intensity field is defined as $|p|^2$. The normalized intensity is $|p/p_0|^2$. In the E-polarization case, p, p_0, and p_s stand for the electric fields E, E_0, and E_s, respectively.

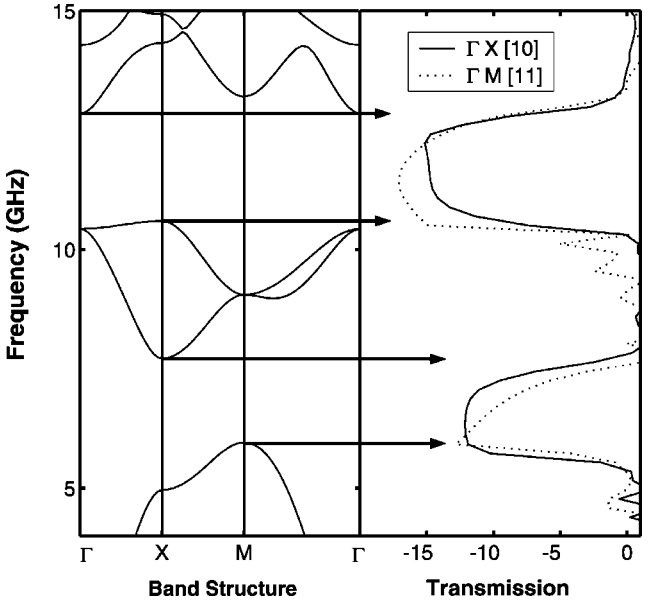

FIG. 1. Left panel: The band structures computed by the plane wave expansion method. Right panel: Here is shown the normalized transmission $\log_{10}|T|^2$ versus frequency; the solid line refers to the result from the [10] direction propagation, and the dotted line to that from the [11] direction propagation lines.

III. RESULTS AND DISCUSSION

In line with most literature, the following parameters are used in the computation. The ratio of the dielectric constant between the cylinders and the hosting medium is 10; the dielectric constant of the medium is taken as one. The filling factor β, the fraction of area occupied by the cylinders per unit area, is 0.28. The radius a of the cylinders is 0.38 cm. The lattice constant d of the corresponding square lattice array of the cylinders is thus about 1.28 cm ($d=a\sqrt{\pi/\beta}$). For convenience, we scale all lengths by the lattice constant d. The computation is continued until the convergence is reached.

First, in Fig. 1 we show the band structure of the corresponding square lattice arrangement of the cylinders, obtained by the plane wave method. The wave transmission in two symmetric directions is also shown. Two complete bandgap regions are identified and are consistent with the highly attenuated regions in the transmission computation. These results are also consistent with that in Fig. 4 of Ref. [4], thereby verifying our numerical scheme.

To investigate wave transmission properties, two situations are considered and compared: (1) Wave propagating through the array of cylinders, labelled hereafter as the "Outside" situation, and (2) wave transmitted from a source located inside the ensemble, labelled hereafter as the ''Inside'' situation. Both cases are illustrated by Fig. 2. For the Outside case, all cylinders are randomly or regularly placed within a rectangular area with length L and width W. The transmitter and receiver are located at some distance from the two opposite sides of the scattering area. For the Inside situation, all cylinders are placed either completely randomly or regularly within a circle of radius L with the source lo-

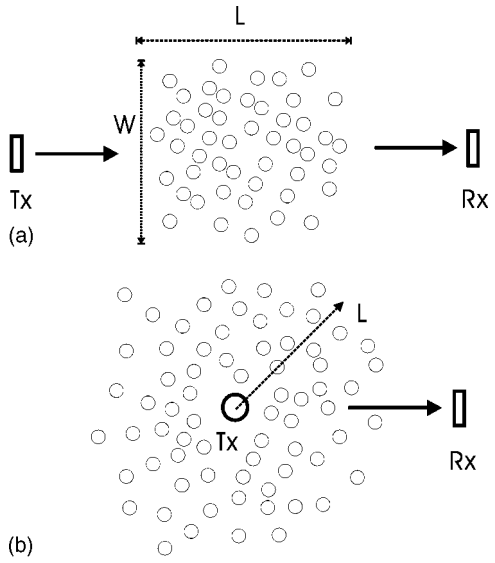

FIG. 2. (a) The Outside case: Electromagnetic propagation through a cloud of dielectric cylinders. (b) The Inside case: Electromagnetic transmission from a line source located inside the array of dielectric cylinders. Here Tx denotes the transmitter, and Rx refers to the receiver.

cated at the center and the receiver located outside the scattering cloud.

The frequency response of the averaged logarithmic transmission is presented in Fig. 3 for both Inside and Outside scenarios. Here we see that the disorder somewhat tends to enhance transmission within the bandgaps for both scenarios, while obviously reduces the transmission for all frequencies outside the gaps in the Outside case. For the Inside situation, however, the reduction for regions outside the gaps is not generally obvious, and is only seen near the gap edges. It has

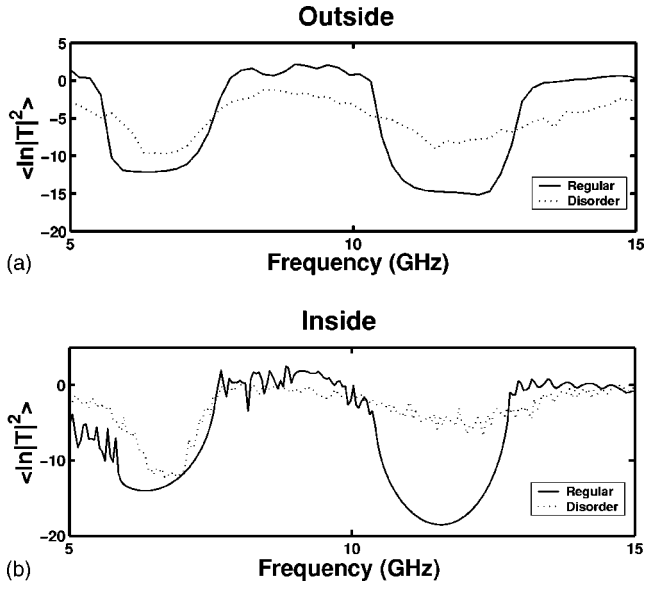

FIG. 3. Transmission versus frequency for both random and regular arrays of cylinders: (a) The Outside case with W=6 and L=10; and (b) the Inside case with L=10. Please refer to Fig. 2 and the text for the explanation about the Outside and Inside cases.

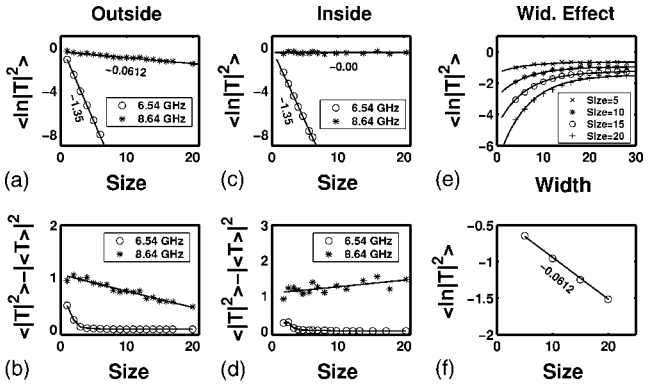

FIG. 4. The averaged logarithmic transmission and its fluctuation versus the sample size for two frequencies: One is within the first bandgap and the other is above the first but below the second gap. The left and center panels refer to the Outside and Inside cases, respectively. The estimated slopes for the transmission are indicated in the figure. The right panel shows the effect of width *W* and the plot of the transmission versus length *L* at the extrapolated infinite width (see the text).

been generally accepted that the transmission reduction in the Outside scenario indicates the onset of localization. Then the intuition is that if the transmission reduction is only caused by the localization effect, it will be implied that the random system only supports localized states. Then waves will not be allowed not only to propagate through but also not to travel when the transmitting source is moved inside the system. Therefore, we would expect the transmission to follow an exponential decay with increasing sample size for both Inside and Outside setups. We would like to examine this intuition.

Figure 4 presents the results for the random ensemble averaged transmission and its fluctuation as a function of the sample size at two frequencies. The sample size is varied by adjusting the number of the cylinders. For the Outside case, we have done the following to remove the effect of the width *W*. With a fixed sample size (i.e., the length *L*), we plot the transmission versus width. We find that the transmission nicely saturates to a certain value in an exponential manner. We have done for several lengths, and obtained the corresponding saturated value for each length. Then we plot these values versus sample lengths. In this way, possible effects of the vertical width may be eliminated. As an example, the results for 8.64 GHz are shown in Figs. 4(e) and 4(f). For 6.54 GHz, the localization is strong, the width effect diminishes very quickly when the width increases. Here the plot for 6.54 GHz has width 26 in the Outside scenario. Note that the width should not be started at a value too close to zero; otherwise the variance will be too large, making the results unstable. The average has been taken for 500 configuration to ensure the stability.

A few important features are discovered. For the frequency of 6.54 GHz (within the first gap), the transmission decays exponentially with the sample size for both Outside and Inside situations with almost the same slope of −1.35. And inside the localization regime, the absolute value of the transmission fluctuation is small, as expected from an earlier work [9,10]. Here we see that within this regime,

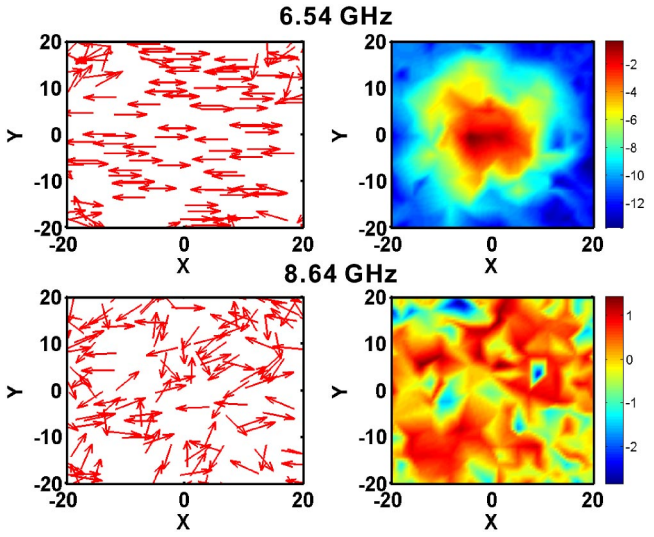

FIG. 5. (Color online). The phase diagram and spatial distribution of electromagnetic energy for two frequencies for one random configuration. Left panel: The phase diagram for the phase vectors defined in the text; here the phase of the direct field E_0 is set to zero. Right panel: the energy spatial distribution.

wave localization can be indeed observed in both Outside and Inside scenarios, and the localization length, inversely proportional to the exponential slope, is consistent in the two situations.

For 8.64 GHz (between the first and the second gaps), the Outside and Inside scenarios differ significantly. For the Outside case the transmission decreases exponentially with a slope of −0.0612 along the path, but such an exponential decay is not obvious in the Inside scenario. The result in the center panel of Fig. 4 clearly shows this point. The fact that the exponential decay only occurs in one scenario but not in the other for the same sample size (L) is itself intriguing and important. Furthermore, as at this frequency, waves are not apparently localized in the Inside case and they have a weaker exponential decay in the Outside case, the transmission will be more sensitive to the arrangement of the cylinders. Therefore the fluctuation at this frequency is stronger than that at 6.54 GHz, as evidenced by the results. However, we note that the ratio between the fluctuation and the transmission at 8.64 GHz could be smaller than that at 6.54 GHz.

Now we discuss a unique feature of EM wave localization. The energy flow of EM waves is $\vec{J} \sim \vec{E} \times \vec{H}$. By invoking the Maxwell equations to relate the electrical and magnetic fields, we can derive that the time averaged energy flow is $\langle \vec{J} \rangle_t \equiv 1/T \int_0^T dt \vec{J} \sim |\vec{E}|^2 \nabla \theta$, where the electrical field is written as $\vec{E} = \vec{e}_E |\vec{E}| e^{i\theta}$, with $\vec{e}_E$ denoting the direction, $|\vec{E}|$ and θ being the amplitude and the phase respectively. It is clear that when θ is constant, at least by spatial domains, while $|\vec{E}| \neq 0$, the flow would come to a stop and the energy will be localized or stored in the space. We assign a unit phase vector, $\vec{u} = \cos\theta_i \vec{e}_x + \sin\theta_i \vec{e}_y$ to the oscillation phase θ_i of the dipoles. Here $\vec{e}_x$ and $\vec{e}_y$ are unit vectors in the x and y directions respectively. These phase vectors are represented by a phase diagram in the x-y plane.

In Fig. 5, the two-dimensional spatial distribution of EM energy ($\sim |E/E_0|^2$) and the phase vectors of the E-field are plotted for the two frequencies discussed in Fig. 4. The phase vectors are located randomly in the x-y plane but to avoid the positions of the cylinders. The Inside scenario is considered. Here we clearly see that for 6.54 GHz, the energy is mainly confined near the source, consistent with Fig. 4. The phase vectors are orderly oriented. These fully comply with the above general discussion. Therefore, at this frequency, EM wave is indeed localized. When we increasingly add an imaginary part to the dielectric constant, the ordered orientation of the phase vectors will disappear, confirming that the phase coherence is a unique feature of EM wave localization. We note from Fig. 5 that near the sample boundary, the phase vectors start to point to different directions. This is because the numerical simulation is carried out for a finite sample size. For a finite system, the energy can leak out at the boundary, resulting in disappearance of the phase coherence. When enlarging the sample size, we observe that the area showing the perfect phase coherence will increase. At 8.64 GHz, however, there is no ordering in the phase vectors $\vec{u}(\vec{r})$. The phase vectors point to various directions. The energy distribution is extended in the x-y plane, and no EM wave localization has been archived yet in this case, in agreement with what has been described for Fig. 4.

From Fig. 3, the fact that the transmission reduction occurs not only within but also outside the gaps (at areas around the edges of the gaps) indicates that the transmission inhibition regions are coincident with the complete bandgaps to certain extends, and these regions seem wider than the gaps. In addition, our results from Fig. 4 show that although the disorders may block waves from propagation *through* the medium in the Outside scenario, but this inhibition may not yet reveal when the source is located inside the 2D medium. This may imply that beside the localization effect, there are other possible causes for the exponential decay in the transmission for the Outside scenario, such as the reflection effect incurred when waves pass across the sample slab, and deflection due to the finite width of the slab. To verify this consideration, we have examined the dependence of the backscattering intensity versus the sample length and width for the two frequencies considered in Fig. 4. The intuition is that the stronger is the backscattering, the weaker will be the transmission.

Figure 6 shows the backscattering intensity versus the sample width for two sample sizes in the Outside case. The frequency is 6.54 GHz. Here we see that as the width is increased, the backscattering intensity increases and will nearly exponentially approach a certain value. The width effect on the backscattering starts to saturate when the width exceeds 20.

In Fig. 7, we plot the backscattering intensity $\langle |E_s|^2 \rangle$ versus sample size for the two frequencies 6.54 and 8.64 GHz in the Outside case. Here we also see that the backscattering increases as the sample size (L) increases and then approaches almost exponentially a certain value for both frequencies; since the width is large enough, the width effect should not be important, as inferred from Fig. 6. Figure 7 also shows that the backscattering at 6.54 GHz is stronger than at 8.64 GHz, indicating that the transmission is weaker

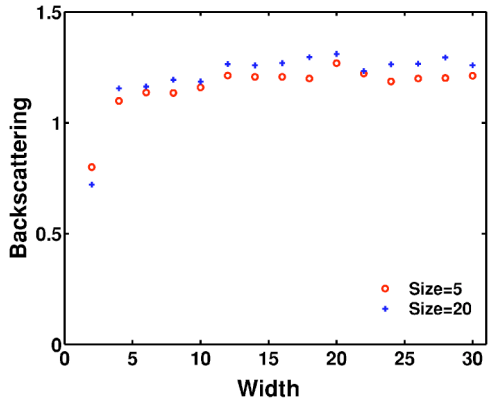

FIG. 6. Backscattering intensity $\langle |E_s|^2 \rangle$ versus sample width for two sample size in the Outside case. The source is placed at 0.5 lattice constant away from the left side of the slab, while the receiver is placed at 3.0 lattice constant away from the left side of the scattering area. The intensity has not been normalized.

at 6.54 GHz than at 8.64 GHz, in agreement with the results in Fig. 4.

While the results in Fig. 6 show that the wave deflection due to the finite width can give rise to the transmission reduction, the results in Fig. 7 clearly indicate that the reflection can also cause the transmission reduction. These results are fully in agreement with that in Fig. 4, thus verifying that the reflection and deflection can lead to the transmission reduction in the Outside case. The reason why the backscattering intensity approaches a certain value when the sample length L or width W increases can be understood as follows. The backscattering intensity is roughly proportional to $1-\langle |T|^2 \rangle$, where T is the normalized transmission. Since $\langle |T|^2 \rangle$ decays exponentially when the width and size increase, as shown in Fig. 4. Therefore, the backscattering intensity will exponentially approach a constant for large widths and sizes, as indicated by Figs. 6 and 7.

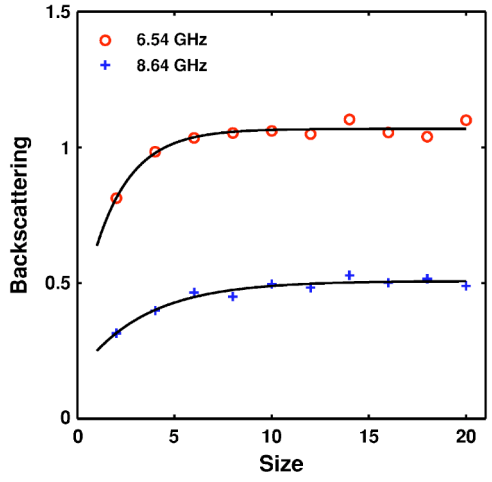

FIG. 7. Backscattering intensity $\langle |E_s|^2 \rangle$ versus sample size for the two frequencies 6.54 and 8.64 GHz in the Outside case. The source is placed at 0.5 lattice constant away from the left side of the slab, while the receiver is placed at 3.0 lattice constant away from the left side of the scattering area. The slab width is 26. The intensity has not been normalized.

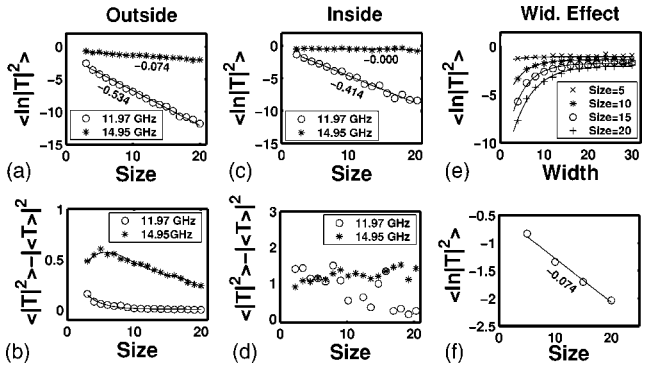

FIG. 8. The averaged logarithmic transmission and its fluctuation versus the sample size for two frequencies 11.97 and 14.95 GHz: One is within the second bandgap and the other is above the second. The left and center panels refer to the Outside and Inside cases, respectively. The estimated slopes for the transmission are indicated in the figure. The right panel shows the effect of width W and the plot of the transmission versus length L at the extrapolated infinite width (see the text).

We have also examined other frequencies. We will show the results for two frequencies in particular: one is within the second gap and the other is above the second gap. The results are very similar to that shown in Figs. 4 and 5, and we present the results in Figs. 8 and 9. The transmission has been averaged over the random configurations of the cylinders. Here, we see that at the frequency of 11.97 GHz (within the second gap), the transmission decays exponentially with the sample size for both Outside and Inside situations. And inside the localization regime, the absolute value of the transmission fluctuation is small. For 14.95 GHz, the Outside and Inside scenarios differ from each other. For the Outside case, the transmission decreases exponentially along the path, but such an exponential decay is not obvious in the

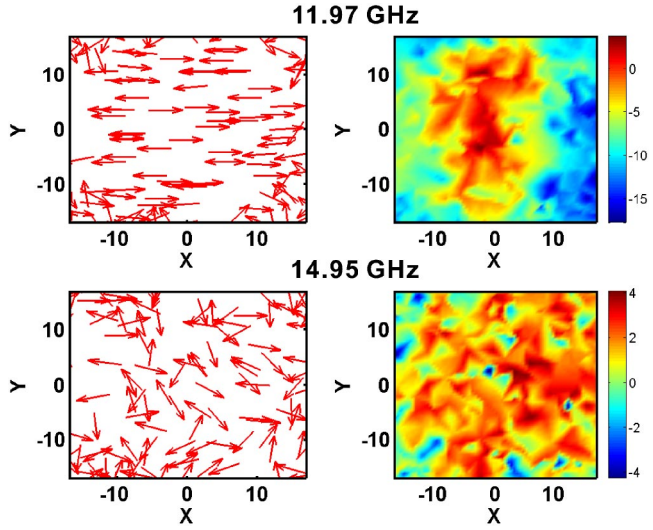

FIG. 9. (Color online). The phase diagram and spatial distribution of electromagnetic energy for two frequencies from Fig. 8 for one random configuration. Left panel: The phase diagram for the phase vectors defined in the text; here the phase of the direct field E_0 is set to zero. Right panel: The energy spatial distribution.

Inside scenario, as shown in the center panel of Fig. 8. As in Fig. 4, the exponential decay at 11.97 GHz is not caused by the width effect. The procedure to exclude the width effect is given above and the result is shown by the right panel of Fig. 8.

In Fig. 9, the two-dimensional spatial distribution of EM energy ($\sim|E/E_0|^2$) and the phase vectors of the E-field are plotted for the two frequencies discussed in Fig. 8. The phase vectors are located randomly in the x-y plane but to avoid the positions of the cylinders. The Inside scenario is considered. Here we clearly see that for 11.97 GHz, the energy is mainly confined near the source, consistent with Fig. 8. The phase vectors are orderly oriented. Therefore, at this frequency, EM wave is localized. At 14.95 GHz, however, there is no ordering in the phase vectors $\vec{u}(\vec{r})$. The phase vectors point to various directions. The energy distribution is extended in the x-y plane, and no EM wave localization has been achieved yet in this case, in agreement with what has been described for Fig. 8.

IV. SUMMARY

In summary, we have examined some fundamental problems of EM wave transmission in 2D random media made of arrays of parallel dielectric cylinders. For the random distribution of cylinders, the transmission is investigated and compared in two scenarios: (1) Wave propagating through the array of cylinders; this is the scenario which has been commonly considered in the literature, and (2) wave transmitted from a source located inside the ensemble. The results indicate that there is a distinct difference between the two situations. It is also shown that the region of the inhibited transmission is related to and seems to be wider than the complete bandgaps. When localized, not only are waves confined near the transmitting source but a unique collective phenomenon emerges.

ACKNOWLEDGMENT

This work was supported by a grant from the National Science Council of the Republic of China awarded to Z.Y.

[1] For a review, please refer to S. John, Phys. Today **40**, 32 (1991); *Scattering and Localization of Classical Waves in Random Media*, edited by P. Sheng (World Scientific, Singapore, 1990); A. Lagendijk and B. A. van Tiggelen, Phys. Rep. **270**, 143 (1996).

[2] Y. Kuga and A. Ishimaru, J. Opt. Soc. Am. A **1**, 831 (1984); M. P. van Albada and A. Lagendijk, Phys. Rev. Lett. **55**, 2692 (1985); P. E. Wolf and G. Maret, *ibid.* **55**, 2696 (1985); A. Tourin *et al.*, *ibid.* **79**, 3637 (1997); M. Torres, J. P. Adrados, and F. R. Montero de Espinosa, Nature (London) **398**, 114 (1999).

[3] M. Rusek and A. Orlowski, Phys. Rev. E **51**, R2763 (1995).

[4] M. M. Sigalas, C. M. Soukoulis, C.-T. Chan, and D. Turner, Phys. Rev. B **53**, 8340 (1996).

[5] D. S. Wiersma, P. Bartolini, A. Lagendijk, and R. Roghini, Nature (London) **390**, 671 (1997).

[6] A. A. Asatryan *et al.*, Phys. Rev. B **57**, 13 535 (1998).

[7] A. A. Chabanov, M. Stoytchev, and A. Z. Genack, Nature (London) **404**, 850 (2000).

[8] F. Scheffold, R. Lenke, R. Tweer, and G. Maret, Nature (London) **398**, 206 (1999); D. Wiersma *et al.*, *ibid.* **398**, 207 (1999).

[9] E. Hoskinson and Z. Ye, Phys. Rev. Lett. **83**, 2734 (1999).

[10] Z. Ye and E. Hoskinson, Appl. Phys. Lett. **77**, 4428 (2000).

[11] V. Twersky, J. Acoust. Soc. Am. **24**, 42 (1951).

[12] Y.-Y. Chen and Z. Ye, Phys. Rev. Lett. **87**, 184301 (2001).